Intracranial Heart Rate Detection Using UWB Radar

Timo Lauteslager*†, Mathias Tømmer‡, Kristian G. Kjelgård‡, Tor S. Lande‡ and Timothy G. Constandinou*†

*Department of Electrical and Electronic Engineering, †Centre for Bio-Inspired Technology, Imperial College London, UK

‡Department of Informatics, University of Oslo, Norway

Email: {t.lauteslager14, t.constandinou}@imperial.ac.uk, {tommer, kristigk, bassen}@ifi.uio.no

Abstract—Microwave imaging is a promising technique for non-invasive imaging of brain activity. A multistatic array of body coupled antennas and single chip pulsed ultra-wideband radars should be capable of detecting local changes in cerebral blood volume, a known indicator for neural activity. As an initial verification that small changes in the cerebrovascular system can indeed be measured inside the skull, we recorded the heart rate intracranially using a single radar module and two body coupled antennas. The obtained heart rate was found to correspond to ECG measurements. To confirm that the measured signal was indeed from within the skull, we performed simulations to predict the time-of-flight of radar pulses passing through different anatomical structures of the head. Simulated time-of-flight through the brain corresponded to the measured delay of heart rate modulation in the radar signal. The detection of intracranial heart rate using microwave techniques has not previously been reported, and serves as a first proof that functional neuroimaging using radar could lie within reach.

Fig. 1. Block diagram of the experimental setup.

I. INTRODUCTION

Non-invasive sensing and imaging of human brain activity is challenging due to the protective skull. Current modalities (EEG, MEG, fMRI, PET, SPECT) are hampered by either high cost, poor temporal or spatial resolution, or the necessity of radioactive tracer fluids. An interesting alternative to functional brain imaging is microwave imaging (MWI). The harmless, non-ionizing microwave signals can penetrate human tissue and may potentially be used to image local changes in impedance in the brain. MWI has been used for remote vital signs monitoring [1], breast cancer detection [2], [3] and stroke detection [4], [5], indicating a blood volume within the brain can be detected using microwaves [4]. Suitable technical solutions for microwave impedance body imaging are limited with most reported MWI systems using vector network analyzers, resulting in long acquisition times. Miniaturized, single-chip ultra-wideband (UWB) pulsed radar technology may provide MWI of brain activity at much higher temporal resolution. A radar here can potentially be used to detect local changes in cerebral blood volume (CBV) [6], as the dielectric contrast between blood and grey matter ($\Delta\epsilon_r$) is significant (relative contrast of 9 at 4 GHz [7]). From MRI studies, it is known that CBV is an indirect indicator for neural activity [8]. Measuring local changes in CBV to detect brain activity is challenging as the signal of interest is of small magnitude, requiring acquisition hardware with high sensitivity. Using signal processing techniques it should be possible to separate the time-varying functional signal from the strong static clutter from structural reflections.

This work is a result of the collaboration between the Centre for Bio-Inspired Technology at Imperial College London, the Dept. of Informatics at the University of Oslo (MEDIMA project) and the Norwegian SME Novelda AS (Ventricorder project). The long ter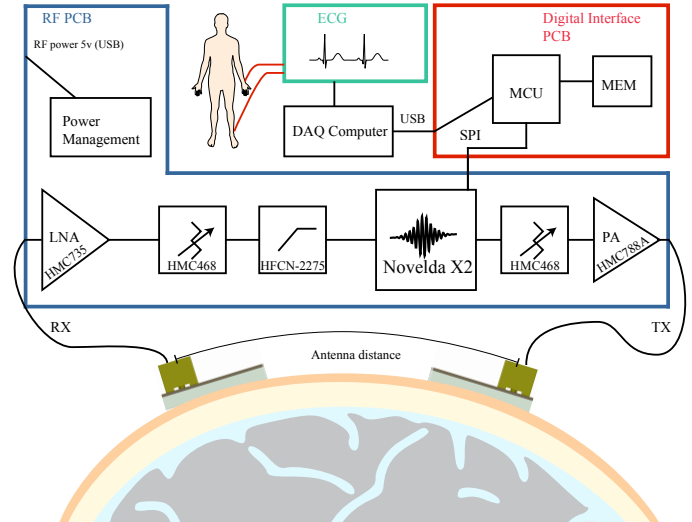m goal is complete brain imaging using coherent imaging radars in a multistatic array covering the head. A smaller array of antennas and radar modules for partial cortical imaging may also be useful. An initial verification that cerebrovascular activity can indeed be measured inside the skull, is to measure intracranial heart rate (HR). To the best of our knowledge, intracranial cardiac activity has not been measured before using MWI techniques.

In this paper we show that the intracranial HR can successfully be detected using an UWB single chip radar and body coupled antennas. The received signals were analysed in the frequency domain and the results were compared to ECG measurements. The dominant frequency found in the received radar signals corresponds to the HR. Simulations of the scenario were used to predict the time-of-flight of the signal of interest, further suggesting that measured HR is indeed from within the skull.

II. METHODS

The experimental setup is illustrated in Fig. 1 with hardware consisting of a radar module (blue) and an ECG recording at 250 Hz between the left and right wrist with right leg drive (green). A digital interface between the radar module and computer (red) controlling the radar module and two body coupled wideband antennas located on the forehead. The measurements were done on a single subject.

A. Experimental setup

The Novelda X2 single chip radar transmits a wideband modulated Gaussian waveform with a -10 dB signal bandwidth of 1.5 – 2.5 GHz and tunable center frequency from 4 – 9 GHz. Using a single bit sampling technique with approximately

40 GHz sampling rate combined with a high pulse repetition rate, good receiver dynamic range and sensitivity is achieved [9]. By reducing the supply voltage, the center frequency was shifted down to 3.8 GHz resulting in a 2 ns long pulse occupying 2.5 GHz signal bandwidth. In terms of power levels the X2 chip is designed to operate with levels in compliance with the FCC regulations (−41.3 dBm/MHz). To achieve a higher SNR, additional amplifiers were added on both transmit and receive paths (Fig. 1), where the transmitted power level was increased by 10 dB. In a simulation study it was found that even in the case of an implantable UWB antenna, up to 13.9 dB could be added without violating SAR/SA limits [10]. Considering the dielectrics of the skull, we are confident not to pose any health threats using the chosen approach. The radar module is a part of the Ventricorder project, a Novelda funded research effort on heart inspection. The antennas used in the experiment are body coupled wideband monopole antennas with a -10 dB impedance bandwidth of 2.5 − 7 GHz, with the antennas placed on the forehead. Using a low loss dielectric spacer with permittivity matching that of the skin ($\epsilon_r \approx 30$), an increased body coupling and reduced performance sensitivity to underlying tissues were achieved. Details on the design, simulations and measurements of the antenna are given in [11].

Using an elastic band the two antennas were pressed against the skin on the forehead with four different distances between the antennas; 60, 80, 100 and 200 mm. For the 200 mm measurement the antennas were positioned in front of the ear superior to the zygomatic arch (cheek bone), which is known as an acoustic window in transcranial Doppler ultrasound, where the skull thickness is sufficiently thin to image some of the basal cerebral arteries.

B. Data analysis

The Novelda X2 radar receiver consists of 256 consecutive samplers with an inter-sampler delay of 25 ps, resulting in a fast-time sampling frequency of 40 GHz. Pulses are transmitted at a PRF of 100 MHz and the receiver integrates each sampler to produce a slow-time frame rate at 80 fps. Fig. 2 illustrates the received data in fast- and slow-time. In fast-time the received signal is a superposition of pulses propagating through multiple paths between the transmit and receive antennas, and due to the complexity of the cerebrovascular system we lack a strong hypothesis on the effect of cardiac activity on the received radar signals in slow-time. Cardiac activity causing arterial dilation inside the brain could result in movement of cerebral tissue. Such a pulsating movement can be observed at the anterior fontanelle, a gap in an infants skull often called the soft spot. A movement of dielectric boundaries within the cranium would give rise to periodic changes in the received radar signal, both in terms of amplitude and phase. Another hypothesis would be that periodic changes in blood volume within the brain result in a periodic change in dielectric permittivity, causing a change in time-of-flight (and therefore phase) of the radar signal.

The first step in analyzing the radar data, is to determine the samplers of interest. That is, the samplers that correspond to a delay in fast-time, at which the signal of interest (path through the brain) can be expected. For this, the HR frequency was determined from ECG data. Next, the slow-time amplitude spectrum was calculated for each sampler, using the chirp
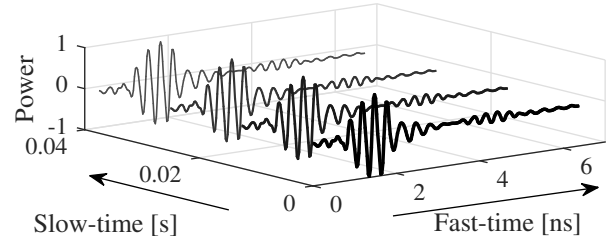

Fig. 2. Illustration of raw radar data, consisting of received signals in fast- and slow-time.

Z-transform. Because we were interested at which samplers the HR would be most prominent, the amplitude at the HR frequency was obtained from the sampler's amplitude spectra. HR amplitude was then plotted over fast-time. By visual inspection, the latest prominent peak was identified as the window containing the signal of interest. 40 Consecutive samplers within this window were chosen as samplers of interest.
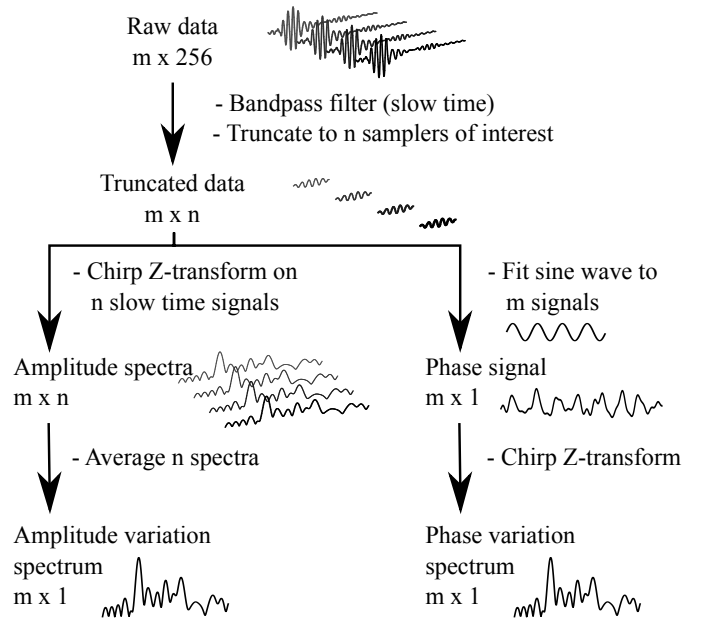

Fig. 3. Signal processing pipeline: The amplitude spectra of the amplitude variation and phase variation are determined from raw radar data, at a set of samplers of interest.

Two approaches were then used to analyse the received radar data at the samplers of interest; average amplitude variations in slow-time and phase variations of the carrier frequency in fast-time. A detailed view of the processing scheme is illustrated in Fig. 3. The slow-time data was bandpass filtered using a zero-phase shift filter with a pass band of 0.8 − 4 Hz. The bandpass filtering removes strong static signals and high frequency noise, leaving in place only the signal that could physiologically be explained by cardiac activity. The slow-time amplitude spectrum was calculated using the chirp Z-transform for each sampler of interest, followed by an averaging over the resulting spectra, yielding an average amplitude spectrum. To study the phase variation a segment of the radar signal was considered as a carrier (single frequency), and its phase was determined as in continuous wave doppler radar. For each slow-time frame a window containing the samplers of interest was selected. Within this window, the relative phase of the

carrier frequency is equal to the angle between the carrier and a sine wave with the same frequency. The phase is thus obtained by taking the arctangent of the inner product between the recorded data and the sine wave with the same frequency and zero phase. After unwrapping the resulting phase signal, the chirp Z-transform was used to obtain the amplitude spectrum of the phase variation of the data.

The amplitude spectrum of the ECG data was calculated, and compared to the amplitude spectra from the amplitude variation and the phase variation of radar data. Because the ECG signal was found to be very noisy, R wave detection was performed and the heartbeat signal was used for frequency analysis instead of the raw ECG data.

C. Time-Domain EM Simulations

Electromagnetic simulations of one of the measured scenarios (200 mm inter-antenna distance) was carried out using a simplified multilayered tissue model of the subject's forehead with dimensions based on the distance between temples and the arc length over the forehead. The tissue model consists of a layer of skin (4 mm), cortical and cancellous bone (1.45 and 3.45 mm), and a heterogeneous mixture of gray matter, white matter, cerebrospinal fluid and blood, where the layer thicknesses were gathered from multiple sources and the dielectric properties from Gabriel et al. [7]. The transient solver in Ansys HFSS was used and the transmit antenna was excited with the same pulse as the one from the X2 radar chip. This way we were able to analyse the different paths via air, skin, bone and brain in the time domain, and verify that the HR signal we measure appears at a delay that corresponds to the signal path propagating through the brain.
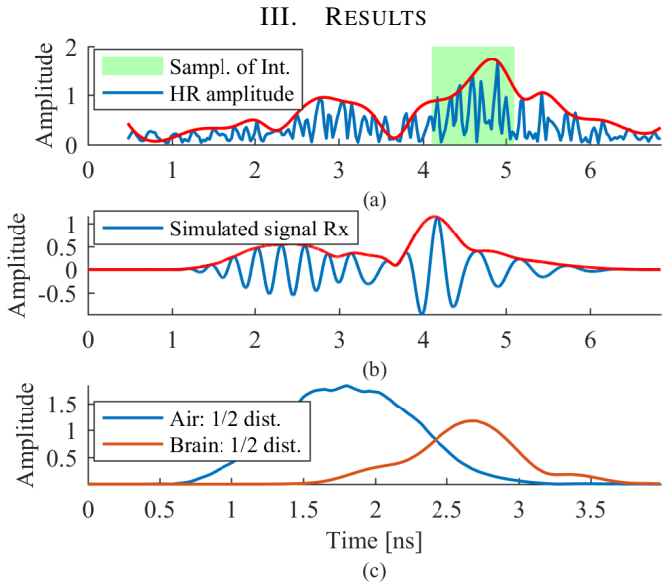
III. RESULTS

Fig. 4. (a) Heart rate Amplitude vs time, (b) Simulated received (static) signal vs time, (c) Simulated half distance field monitors (envelope) mid brain and in air (center of the model). Envelopes are added for clarity in a and b.

Fig. 4 shows the measured HR frequency amplitude as a function of time delay for the 200 mm inter-antenna distance, as well as results from the time-domain simulation of the 200 mm scenario, with the envelope of the signals added for clarity. The simulated received signal (Fig. 4b) is

a superposition of the multiple paths that the radar pulse propagates through: the low velocity path directly through the brain, the high velocity path over air, and several other smaller contributions from the skin and skull layers of the model. Our initial hypothesis was that the first part of the signal (1.5 – 3 ns) is mainly the air wave, followed by signal contributions from within the head. To verify that the pulse arriving between 4 – 4.5 ns is the one going straight through the brain, field monitors were placed in the middle of the different layers (at half the total path length) of the simulation model. This way the multiple contributions seen at the receiver were isolated, making it possible to predict the delay of individual paths. The amplitude measured at the field monitors in the brain and in air are shown in Fig. 4c. Note that the range of the time axis is half that of Fig. 4b, as we consider half the path length. Comparing these simulation results to measurement results (Fig. 4a), we find that all three graphs predict two distinct peaks. The measured HR amplitude shows a strong peak at 4 – 5 ns, which corresponds well to the simulated brain wave in the field monitors, but is slightly later than the second peak in the received signal. The earlier peak in HR amplitude (2.5 – 3.5 ns) appears to be well explained by the air wave in simulation results.

Repeating the measurement with the antennas separated with a distance of 60, 80, 100 and 200 mm, the HR amplitude as a function of time delay was calculated to estimate the samplers of interest, which were required for the next analysis step. The results are shown in Fig. 5 with the samplers of interest marked in green. Amplitude spectra from radar amplitude variation and radar phase variation at the samplers of interest are then given for different antenna positions in Fig. 6, along with the ECG spectra. In general, there is an excellent correspondence between the dominant frequencies of both radar analyses with the HR of the ECG signal, with the phase variation spectrum at antenna distance of 60 mm being the only exception. The strong peaks in the ECG amplitude spectrum at multiples of the fundamental frequency are harmonics, and occur due to the usage of the heartbeat signal instead of the raw ECG data.
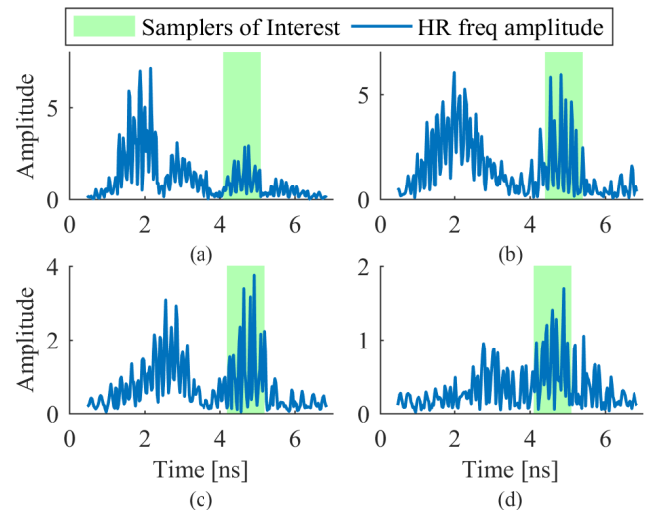

Fig. 5. Amplitude of the heart rate frequency (∼1.2 Hz) in radar data, for antenna distances of: (a) 60 mm; (b) 80 mm; (c) 100 mm; and (d) 200 mm. The 40 samplers of interest are marked in green, and correspond to the latest segment where the heart rate frequency is visually prominent.
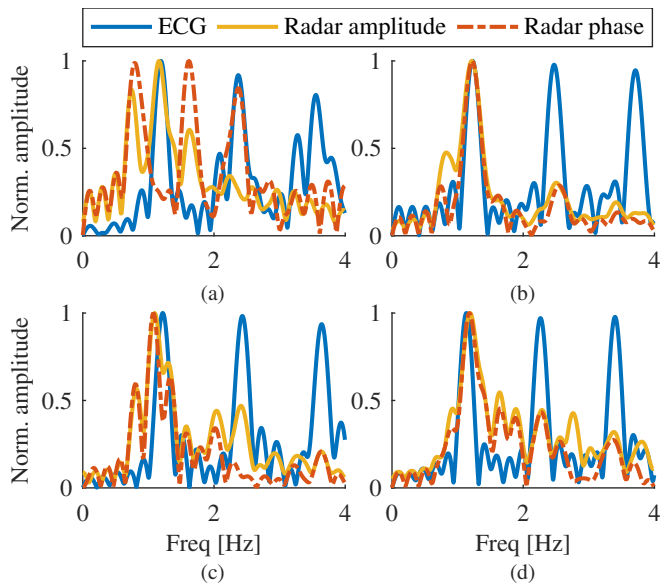
Fig. 6. Normalized amplitude spectra of ECG, radar amplitude variation and radar phase variation for antenna distances of: (a) 60 mm; (b) 80 mm; (c) 100 mm; and (d) 200 mm. With one exception, all data show a dominant peak at the heart rate frequency (∼1.2 Hz), and excellent correspondence between the ECG data and radar data. Strong harmonics in the ECG spectrum are present due to the use of a heart beat signal instead of raw ECG data.

IV. DISCUSSION

The results demonstrate that it is possible to measure intracranial HR using a single chip pulsed UWB radar along with body coupled antennas. With the antennas located on the temples, the received signal passing through the brain gets amplitude modulated by cardiac activity in slow-time. Additionally the time-of-flight and thereby the phase of the received signal is affected by cardiac activity. Both effects occurred at the same frequency as the HR, validated by ECG. In the current experiment, two different analyses were applied on the raw radar data, based on different hypotheses of how cardiac activity influences the radar signal. Although both methods were effective, future measurements (including more participants) could point out differences in performance.

Through the simulation results we were able to determine that the strongest peak in Fig. 4 originates from within the brain. The earlier observed peaks can most likely be explained by the path through air, which has a much higher propagation speed. A question that remains unanswered is how the air wave gets modulated at the HR frequency. We currently have multiple hypotheses on this: One possible explanation could be that sub-mm movements of the skin surface due to cardiac activity result in a slightly longer propagation path around the forehead in air, causing a time shift of carrier wave between slow-time frames. A second possible explanation could be that parts of the air wave creep into the skin. The skin contains arteries, which could cause both skin movement and a change in blood fraction, changing the dielectric permittivity of the skin. Through interference of the path through air and paths propagating partially through tissue, the powerful air wave could be affected by cardiac activity.

As can be observed in Fig. 5, changing the antenna distance increases the path length through air, thus the time delay of the first peak. The latest prominent peak however, the one we

argue to originate from propagating through the brain, seems to occur at a rather consistent delay. Whereas in the 200 mm measurement we rely on transmissive radar measurements, in case of the 60, 80 and 100 mm antenna distance we expect mainly reflected energy. The observed delay corresponds to a depth of approximately 9 cm, indicating that deeper structures in the brain are also being sensed. The cerebral basal arteries could be considered a plausible candidate, but future measurements using multistatic radar should point out the location of the scatterer. In the current work we did not include simulations of the 60, 80 and 100 mm scenario, as the short antenna distance in combination with the pulse length made it difficult to isolate contributions from different paths.

V. CONCLUSION

MWI could potentially be used as a diagnostic tool for cerebrovascular conditions. Blood flow in the cerebral basal arteries is commonly measured using ultrasound techniques. Although radar has a lower spatial resolution than ultrasound, the improved tissue penetration in combination with source localization (using an array of antennas) could make for a complementary diagnostic technique. However, the importance of the current work lies in the fact that this is the first reported measurement of intracranial HR, using MWI. Our long term goal is to detect changes in CBV using multistatic radar, as an indicator for neural activity. Considering this, the detection of intracranial HR serves as the first evidence that cerebrovascular activity can be measured using radar, showing that functional neuroimaging could lie within reach.

REFERENCES

[1] L. Ren *et al.*, "Noncontact heartbeat detection using uwb impulse doppler radar," in *BioWireleSS, 2015 IEEE Topical Conf.*, 2015, Conference Proceedings, pp. 1–3, [Online].

[2] P. Meaney *et al.*, "Microwave imaging for neoadjuvant chemotherapy monitoring: initial clinical experience," *Breast Cancer Res*, vol. 15, no. 2, pp. 1–16, 2013, [Online].

[3] E. Fear *et al.*, "Microwave breast imaging with a monostatic radar-based system: A study of application to patients," *Microwave Theory and Techniques, IEEE Trans.*, vol. 61, no. 5, pp. 2119–2128, 2013, [Online].

[4] M. Persson *et al.*, "Microwave-based stroke diagnosis making global prehospital thrombolytic treatment possible," *Biomedical Engineering, IEEE Trans.*, vol. 61, no. 11, pp. 2806–2817, 2014, [Online].

[5] A. Mobashsher *et al.*, "Design and experimental evaluation of a non-invasive microwave head imaging system for intracranial haemorrhage detection," *PLoS ONE*, vol. 11, no. 4, p. e0152351, 2016, [Online].

[6] T. Lauteslager *et al.*, "Functional neuroimaging using ultra-wideband impulse radar," *Biomedical Circuits and Systems Conference (BioCAS), 2015 IEEE, 22-24 Oct.*, 2015, [Online].

[7] S. Gabriel *et al.*, "The dielectric properties of biological tissues: Iii. parametric models for the dielectric spectrum of tissues," *Phys. in med. and biology*, vol. 41, no. 11, p. 2271, 1996, [Online].

[8] S.-G. Kim *et al.*, "Cerebral blood volume mri with intravascular superparamagnetic iron oxide nanoparticles," *NMR in Biomedicine*, vol. 26, no. 8, pp. 949–962, 2013, [Online].

[9] H. Hjortland and T. Lande, "Ctbv integrated impulse radio design for biomedical applications," *BioCAS, IEEE Trans.*, vol. 3, no. 2, pp. 79–88, 2009, [Online].

[10] K. Thotahewa *et al.*, "Sar, sa, and temperature variation in the human head caused by ir-uwb implants operating at 4 ghz," *IEEE Trans. on Microwave Theory and Techniques*, vol. 61, no. 5, pp. 2161–2169, 2013, [Online].

[11] M. Tømmer *et al.*, "Body coupled wideband monopole antenna," *Loughborough Antennas & Propagation Conference, 2016 IEEE*, Nov. 2016, in press.